

Ferromagnetic metal to cluster-glass insulator transition induced by A-site disorder in manganites

K. F. Wang, Y. Wang, L. F. Wang, S. Dong, H. Yu, Q. C. Li, and J.-M. Liu^{a)}

Laboratory of Solid State Microstructures, Nanjing University, Nanjing 210093, China and International Center for Materials Physics, Chinese Academy of Sciences, Shenyang 110016, China

Z. F. Ren

Department of Physics, Boston College, Chestnut Hill, Massachusetts 02467

(Received 9 November 2005; accepted 15 March 2006; published online 12 April 2006)

The magnetotransport behaviors of a series of rare earth manganites with the same A-site cational mean radius and different A-site ionic radii variance (A-site disorder) are investigated. It is found that the system's ground state transforms from ferromagnetic metal to cluster-glass insulator with increasing A-site disorder. In the cluster-glass state, the magnetization shows the steplike behavior, indicating the existence of short-range magnetically ordered clusters. The significant effect of the A-site disorder on the electronic phase separation is revealed by detecting the cluster-glass ground state at low temperature. © 2006 American Institute of Physics. [DOI: 10.1063/1.2194826]

Perovskite manganites ($AMnO_3$) have been attracting attentions not only for the potential applications due to the colossal magnetoresistance^{1–3} (CMR) that can be understood in the framework of double exchange (DE) model,⁴ but also for the fundamental understanding of the magnetic orders and the associated phase transitions. It has been recognized that the electronic phase diagram of CMR manganites is multicritical, involving competitions of spin, charge or orbital, and lattice orders,^{5,6} leading to electronic phase separation and inhomogeneous electronic and magnetic ground states.^{2,7} At the same time, the significance of intrinsic disorder in manganites has also been recognized. For example, in $Ln_{0.5}Ba_{0.5}MnO_3$, rare earth Ln and Ba ions can form an ordered or disordered structure causing a significant disordered effect.⁸ The disorder can result in glassy ground state and enhance the fluctuations of the order competitions, i.e., between the charge-ordered-orbital ordered (CO–OO) state and ferromagnetic metal (FMM) state, near the original bicritical point. Such fluctuations are amenable to an external magnetic field. Therefore, applying a field favors the FMM phase and produces the CMR effect.

It has been reported that the variance of the A-site ionic radii, $\sigma^2 = \sum_i x_i r_i^2 - \langle r_A \rangle^2$, where x_i and r_i are the atomic fraction and ionic radii of i -type ions at A-site, respectively, is a key parameter to describe the A-site disorder and has significant influence on the magnetic and transport properties of manganites.^{9,10} The A-site cational size mismatch can induce A-site disorder over a wide range but not causing distortion of the lattice structure. Therefore, an investigation of the A-site disorder can provide us additional clues to understand the CMR effect in manganites. Even though some earlier studies reported the relevance between ferromagnetic Curie point T_C and the A-site disorder in some manganites,^{9,10} there was not much work on the effect of the A-site disorder on neither the phase separation nor the inhomogeneity. It was postulated that the A-site disorder may lead to electronic and magnetic disordering effects, such as cluster-glass behavior, electronic localization, and so on. In this letter, we report the effects of A-site disorder on the phase separation and particu-

larly the ground state transition from metal to glassy insulator.

In our experiments, we prepared a series of samples with the same A-site cational mean radius $\langle r_A \rangle = 1.20 \text{ \AA}$ but different variance σ^2 from 0.003 to 0.015, as shown in Table I. Both the $\langle r_A \rangle$ and σ^2 were calculated using standard nine-coordinated cational radii.¹¹ These samples were sintered by the conventional solid-state reaction in air. High-resolution x-ray diffraction (XRD) with Cu $K\alpha$ radiation was performed on these samples at room temperature. The transport measurements were performed using a standard four-probe method with temperature (T) in 20–300 K. The magnetizations of zero-field cooling (ZFC) and field cooling (FC) were measured as a function of T and magnetic field (H) using a Quantum Design superconducting quantum interference device (SQUID) magnetometer. The magnetic loops from $H=0$ to 7 T were recorded at 3 K.

The XRD patterns of all the samples are presented in Fig. 1. All the peaks can be indexed with a single orthorhombic structure with space group $Pbnm$. There was no measurable peak shift for samples with different σ^2 , indicating essentially the same lattice parameters for all the samples. It is estimated that the volume change corresponding to the variation of σ^2 from 0.003 to 0.015 is less than 0.5%. The curves of zero-field resistivity (ρ) as a function of T for all the samples are plotted in Fig. 2(a). It is clearly shown that ρ is very much dependent on σ^2 . In general, at a given temperature, ρ increases with σ^2 , whereas at given σ^2 , different $\rho \sim T$ behaviors were observed. For $\sigma^2=0.003$, ρ exhibited a

TABLE I. Summary of chemical, structural, and physical data for the $RE_{0.55}AE_{0.45}MnO_3$ series with a constant A-site cation mean radius $\langle r_A \rangle = 1.20 \text{ \AA}$.

Chemical composition	σ^2 (\AA^2)	T_{MI} (K)	T_C (K)	T_f (K)	$M(T=3 \text{ K})$ ($\mu_B/f.u.$)
$Nd_{0.55}(Ca_{0.45}Sr_{0.55})_{0.45}MnO_3$	0.003	~197	~194		3.36
$Sm_{0.55}(Ca_{0.2}Sr_{0.8})_{0.45}MnO_3$	0.007	~100	~115		2.82
$Nd_{0.55}(Ca_{0.76}Ba_{0.24})_{0.45}MnO_3$	0.008			~42	2.62
$Gd_{0.55}Sr_{0.45}MnO_3$	0.009			~42	1.51
$Sm_{0.55}(Ca_{0.6}Ba_{0.4})_{0.45}MnO_3$	0.015			~42	1.01

^{a)} Author to whom correspondence should be addressed; electronic mail: liujm@nju.edu.cn

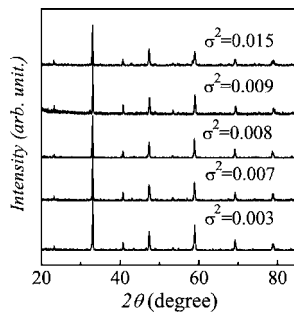


FIG. 1. XRD θ - 2θ spectra measured at room temperature for the samples with $\sigma^2=0.003, 0.007, 0.008, 0.009,$ and $0.015,$ respectively.

metal-insulator transition (MIT) at $T \sim 197$ K (T_{MI}).² With σ^2 increased to 0.007, the MIT occurred at ~ 100 K. When $\sigma^2 \geq 0.008$, there was no MIT observed down to 20 K, meaning that the samples remained to be insulating.

Figure 3 presents the T dependence of magnetization (M). The samples with $\sigma^2=0.003$ and 0.007 exhibited a paramagnetic (PM)-FM transition at (define T_C) $T_C \sim 194$ and ~ 115 K, respectively, roughly in agreement with the MIT shown in Fig. 2. For $\sigma^2 > 0.008$, the M - T curves (ZFC) showed a cusplike peak at $T=T_f \sim 42$ K. The irreversibility between the ZFC and FC M - T curves is very clear. These phenomena allow us to argue that a cluster-glass transition is probably occurring at T_f . In fact, similar results for $\text{La}_{2/3}\text{Ca}_{1/3}\text{MnO}_3$ doped with either Ga or Al or Fe were previously reported.^{12,13}

The M - H curves at $T=3$ K are shown in Fig. 4. For $\sigma^2=0.003$ and 0.007 , saturated M is reached at $H=1$ T, whereas for $\sigma^2=0.008$ M remains unsaturated till 3.5 T, at which a stepwise behavior occurred. For $\sigma^2=0.009$ and 0.015 , M remains unsaturated even at 6.0 T.

It is well known that if all the Mn ions in the samples were ferromagnetically aligned, the maximum spin-only moment is $3.55\mu_B/\text{f.u.}$ However, the measured M at 3 K and 3 T decreased from 3.36 to $1.01\mu_B$ as σ^2 increased from

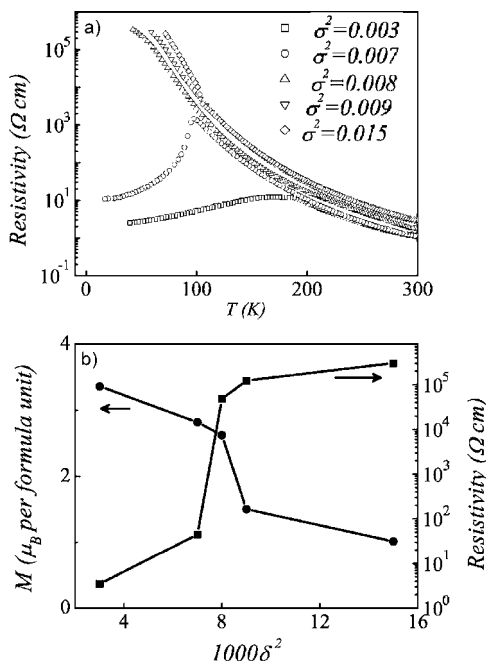


FIG. 2. (a) Measured ρ - T relations for the samples with σ^2 from 0.003 to 0.015; (b) σ^2 dependences of M measured at $T=3$ K under $H=3$ T and σ^2 dependences of zero field ρ measured at $T=50$ K.

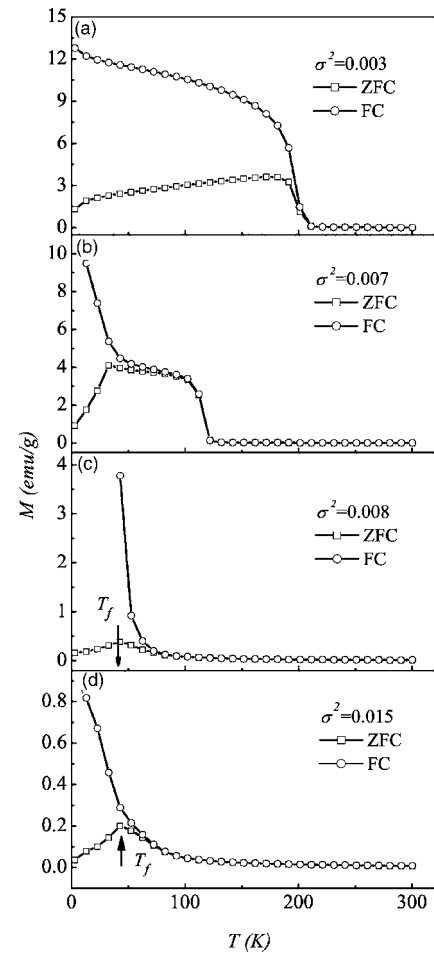


FIG. 3. Measured M - T relation under ZFC and FC conditions for the samples with (a) $\sigma^2=0.003,$ (b) $0.007,$ (c) $0.008,$ and (d) $0.015,$ respectively. The arrows in (c) and (d) indicate the cluster-glass transition point.

0.003 to 0.015, shown in Table I and Fig. 2(b), with an abrupt decrease occurred at $\sigma^2 \sim 0.008$. Simultaneously, the zero field ρ increased significantly at $\sigma^2=0.008$ [Fig. 2(b)], which is the reflection of a MIT induced by electron local-

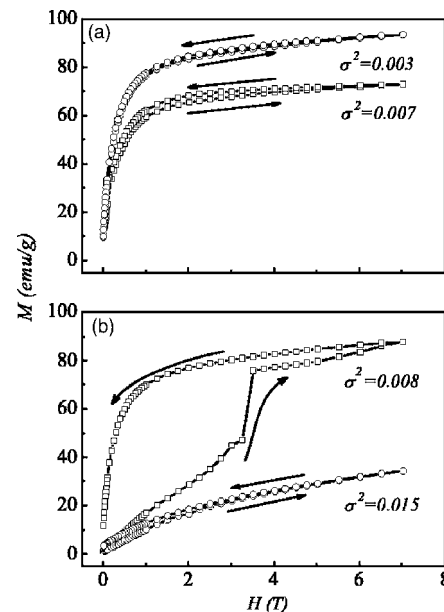


FIG. 4. Measured M - H curves at $T=3$ K, for the samples with (a) $\sigma^2=0.003$ and 0.007 and (b) 0.008 and $0.015,$ respectively. The arrows indicate the variation of H during measurements.

ization. We argue that the increased σ^2 induced the electron localization and enabled ground state transition from FMM to cluster-glass-like insulator. The detailed properties of the cluster-glass state will be reported elsewhere.¹⁴ To understand the physics underlying the cluster-glassy transition, one may consider the scenario of phase separation in response to the *A*-site disorder and magnetic field. The DE interaction responsible for FMM state is scaled by single electron bandwidth W .¹⁵ The FMM state is destabilized in distorted manganites, and often replaced by phases competing against FMM, such as CO–OO antiferromagnetic (AFM) insulator (AFI). A typical case is that the reduction of the *A*-site radius leads to ordered oxygen displacement and thus a CO–OO AFI. In addition, the size difference between the neighboring *A*-site R^{3+} and M^{2+} ions around one oxygen ion (i.e., *A*-site size mismatch) may enable the random oxygen displacement and consequently a local distortion of MnO_6 octahedra.

Since all the samples in the present study have the same $\langle r_A \rangle = 1.20 \text{ \AA}$, very close to the ideal value, they have the same bandwidth W . The sample with small σ^2 ($=0.003$) certainly exhibits the typical MIT (FM-PM transition). As the *A*-site disorder increases ($\sigma^2 \leq 0.007$), the oxygen displacements and the radial distortions of the MnO_6 octahedra are random because the *A*-site ions randomly distribute in the lattice, which keeps the macroscopic structure unchanged. The Mn ions around the distorted MnO_6 octahedra may no longer be able to participate in the DE process. Moreover, considering the fact that the ground state in distorted manganites is often the CO–OO AFI rather than FM state, it is reasonable to argue that the distorted MnO_6 octahedra induced by *A*-site disorder prefers a locally short-ranged CO–OO AFI state. Although FM and CO–OO AFI phases coexist, the FM phase is dominant.

When $\sigma^2 \sim 0.008$, an intermediate disordered state, the system has more CO–OO AFI phase than the FM phase, and electron localization happens evidenced by the insulating behaviors over the whole T range. In such a case, a magnetic field favors the FM phase expansion at the expense of the AFI phase. Subsequently, the expansion of the FM phase requires H to be higher than a critical value in order for the Zeeman energy to overcome the strain energy. At this critical field, a sharp magnetization step is observed, as shown in Fig. 4(b) ($\sigma^2 = 0.008$). This steplike effect indicates the coexistence of the long-range FM regions and the short-range CO–OO AFI regions in the sample.

As $\sigma^2 > 0.008$, it is argued that the long-range FM ordering is completely broken, and the short-range regions become dominant. This corresponds to the so-called cluster-glass state. The magnetization M is small ($M \sim 1.01 \mu_B$ at 4.0 T for the sample of $\sigma^2 = 0.015$). If this argument applies, the ρ - T relation can be described by the variable-range-hopping (VRH) model:¹⁶ $\rho = \rho_{i0} \exp[(T_0/T)^{1/4}]$, where ρ_{i0} is the prefactor and T_0 is the characteristic temperature. Otherwise, the small polaron mechanism will apply above T_{MI} .² In fact, for $\sigma^2 \geq 0.007$ the ρ - T relation above T_{MI} does follow the VRH model rather than the small polaron one. The good linear behavior apart from very low T indicates that the *A*-site disorder favors the electron localization and the cluster-glass state.

Earlier theoretical work dealt with the effect of quenched disorder on the electronic phase separation by first-order

transitions, which corresponds to a phase diagram with features resembling the quantum critical behavior. The low- T region consists of coexisting ordered clusters.^{17,18} Generally, in manganites, the DE interaction and AFM superexchange interaction favor the long-range FM and AFI orders, respectively. For a coexisting two-phase system, an intermediate disorder often brings forth a MIT transition. Our experimental results seem to confirm the prediction of Tokura and Nagaosa,² Burgy *et al.*,¹⁷ and Sen *et al.*¹⁸ that the competition of two opposite interactions plus quenched disorder will favor a cluster-glass state, which may be induced by the enhanced quantum fluctuations between the competing interactions as the consequence of the quantum phase transition. Therefore, the disorder-induced quantum fluctuation is probably one of the important ingredients of the CMR physics, although more direct and dynamic evidence is needed, which is being studied.

In conclusion, we have investigated the effect of the *A*-site disorder on the magnetic and transport behaviors of perovskite CMR manganites by changing the *A*-site cation size. It has been observed that the increasing of *A*-site disorder results in the transition of the ground state from metal to insulator because of the electron localization. The long-range FM state preferred with $\sigma^2 < 0.007$ is replaced by the cluster-glass state with $\sigma^2 < 0.009$. At $\sigma^2 \sim 0.008$, the coexistence of the two states has been revealed. Our results agree with the previous theoretical prediction and reveal the essential role of the *A*-site disorder in the CMR physics.

This work was supported by the Natural Science Foundation of China (50332020, 50528203, and 10021001) and the 973 Projects of China (2002CB613303). One of the authors (J.M.L.) acknowledges the support of Hong Kong Polytechnic University through project (B-Q552).

- ¹S. Jin, T. H. Tiefel, M. McCormack, R. A. Fastnacht, R. Ramesh, and L. H. Chen, *Science* **264**, 413 (1997).
- ²Y. Tokura and N. Nagaosa, *Science* **288**, 462 (2000).
- ³E. Dagotto, T. Hotta, and A. Moreo, *Phys. Rep.* **344**, 1 (2001).
- ⁴C. Zener, *Phys. Rev.* **82**, 403 (1951).
- ⁵A. J. Millis, P. B. Littlewood, and B. I. Shraiman, *Phys. Rev. Lett.* **74**, 5144 (1995).
- ⁶S. Murakami and N. Nagaosa, *Phys. Rev. Lett.* **90**, 197201 (2003).
- ⁷M. Uehara, S. Mori, C. H. Chen, and S.-W. Cheong, *Nature (London)* **399**, 560 (1999).
- ⁸D. Akahoshi, M. Uchida, Y. Tomioka, T. Arima, Y. Matsui, and Y. Tokura, *Phys. Rev. Lett.* **93**, 177203 (2003).
- ⁹L. M. Rodriguez-Martinez and J. Paul Attfield, *Phys. Rev. B* **54**, R15622 (1996).
- ¹⁰L. M. Rodriguez-Martinez and J. Paul Attfield, *Phys. Rev. B* **58**, 2426 (1998).
- ¹¹R. D. Shannon, *Acta Crystallogr., Sect. A: Cryst. Phys., Diffr., Theor. Gen. Crystallogr.* **32**, 751 (1976).
- ¹²J. M. De Teresa, P. A. Algarabel, C. Ritter, J. Blasco, M. R. Ibarra, L. Morellon, J. I. Espeso, and J. C. Gómez-Sal, *Phys. Rev. Lett.* **94**, 207205 (2005).
- ¹³J. Blasco, J. García, J. M. de Teresa, M. R. Ibarra, J. Perez, P. A. Algarabel, C. Marquina, and C. Ritter, *Phys. Rev. B* **55**, 8905 (1997).
- ¹⁴K. F. Wang, Y. Wang, L. F. Wang, S. Dong, D. Li, and Z. D. Zhang, H. Yu, Q. C. Li, and J.-M. Liu (unpublished).
- ¹⁵N. Furukawa, *J. Phys. Soc. Jpn.* **64**, 2734 (1995).
- ¹⁶N. Mott, *Conduction in Non-Crystalline Materials* (Clarendon, Oxford, 1993).
- ¹⁷J. Burgy, M. Mayr, V. Martin-Mayor, A. Moreo, and E. Dagotto, *Phys. Rev. Lett.* **87**, 277202 (2001).
- ¹⁸C. Sen, G. Alvarez and E. Dagotto, *Phys. Rev. B* **70**, 064428 (2004).